

Small Payload Transfers from Earth to LEO and LEO to Interplanetary Space using Lasers

C. Phipps*, C. Bonnal**, F. Masson**, M. Boustie⁺, L. Berthe⁺⁺, S. Baton[§], E. Brambrink[§], J.-M. Chevalier^{§§},
L. Videau[¶], S. Boyer[‡] and M. Schneider⁺⁺

*Photonic Associates, LLC

200A Ojo de la Vaca Road, Santa Fe NM, USA 87508

**CNES, Direction des Lanceurs

52 rue Jacques Hilaret, 75612 Paris Cedex, France

⁺CNRS-Université Poitiers, Poitiers, France

⁺⁺CNRS-Arts et Metiers ParisTech, Paris, France

[§]LULI, École Polytechnique, Palaiseau, France

^{§§}CEA, DAM, CESTA, Paris, France

[¶]CEA, DAM, DIF, Paris, France

[‡]Mines ParisTech, CEMEF, Paris, France

Abstract

Recently, we obtained data on several materials at 80ps pulse duration and 1060nm wavelength which give us the option of proportionally combining them to obtain any value we want for momentum coupling coefficient C_m , from 35 (aluminum) to 800N/MW (POM, polyoxymethylene). Laser ablation physics lets us transfer to LEO or from LEO to interplanetary space using repetitively pulsed lasers and C_m values appropriate for each mission. We discuss practical results for lifting small payloads from to LEO, and space missions such as a cis-Mars orbit with associated laser system parameters.

1. Propulsion by Light

The physics of small payload transfers from Earth to low Earth orbit (LEO) using laser ablation propulsion concepts, as well as for laser propulsion in space were considered in some detail in earlier work [1,2]. There are many other applications for this technology in space [3]. We predicted that costs of small-target transfers to LEO using this technique could be far below today's \$10,000/kg with multiple launches per day. Missing from these early reports was data on particular ablation materials giving practical values of C_m . The history of photon propulsion begins ninety years ago with Tsander [4], Tsiolkovsky [5] and Oberth [6], leading to today's "solar sails." In 1953, Sänger published his concept for photon rockets [7] well before the invention of lasers.

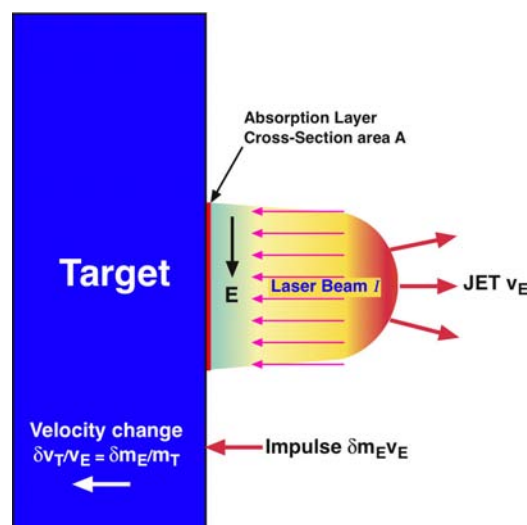


Figure 1. Laser ablation impulse generation

For usefully large forces - for example, enough to counteract gravity or accelerate a several-kg object to orbital speeds in a reasonable time, pure photon propulsion is too weak, and laser ablation propulsion is more attractive.

Laser ablation propulsion operates, ideally in vacuum, by inducing a jet of vapor and plasma from a target using a laser pulse, which transfers momentum to the target (Figure 1) [8]. Terminology is explained in more detail in our review of the field [9].

2. Purpose of this Paper

The purpose of this paper is to update the reference [2] analysis of laser ablation propulsion into low Earth orbit (LEO), and to extend the analysis to interplanetary transfers at much higher velocity using new impulse coupling data we recently obtained at École Polytechnique. We first briefly review the physics and history of this field, then discuss the two applications. When mission duration is at a premium and laser energy is not, we will show that C_m as low as 70N/MW is a good optimum for getting from LEO to Mars and 100-150N/MW from ground to LEO.

3. Laser Momentum Transfer Physics

The laser impulse coupling coefficient C_m is the ratio of momentum delivered to a target by an ablation jet to the incident beam energy W for a laser pulse, or of surface pressure to incident intensity,

$$C_m = m_T \delta v_T / W = \delta \mu_E v_E / \Phi = p / I . \quad (1)$$

In Eq. (1), m_T is target mass, p is surface pressure at the target, I is intensity (W/m^2), $\Phi = I\tau$ is fluence on target (J/m^2), v_E is exhaust velocity of the laser ablation jet and $\delta \mu_E$ is areal mass density (kg/m^2) in the ablation jet column created by one pulse. C_m has dimensions N-s/J or N/W. C_m for pure-photon pressure is minute: the “momentum coupling coefficient” for pure radiation reflecting off a polished surface is

$$C_m = 2/c = 6.7 \text{ mN/MW} . \quad (2)$$

A 10-kW laser reflecting perfectly off a surface would produce a thrust of only 67 μ N. The other important parameter for any type of photon propulsion is propellant exit velocity, v_E , simply c for light, but $(2kT_i / m_i)^{1/2} \ll c$ for laser ablation propulsion. T_i and m_i are ion temperature and mass.

Conservation of energy says that the efficiency of the whole process is

$$\eta_{AB} = \psi C_m v_E / 2 . \quad (3)$$

The parameter $\psi \approx 1$, as we discuss after Eq. (4).

For very long trips, where time is available, solar sails represent a practical use of pure photon propulsion, taking advantage of the fact that, for light in reflection, $I_{sp} = c/g_0$, a very large number. The Eq. (2) value for the C_m of light arises from the fact that the energy density of light I/c is doubled on reflection. At 1kW/m² at our distance from the Sun, a 10-km diameter reflective sail will generate 520N thrust. Using this thrust, a 2 μ m, 250-ton Al-coated plastic reflective film with this diameter could accelerate to 3 km/s in 17 days. The main problem is how to deploy such a film. Despite decades of development, the largest sail yet deployed (JAXA IKAROS [10], 2010) is 14x14m.

Variable v_E can be achieved by adjusting laser intensity on target – by changing focal spot area, laser pulse duration and energy – which causes exhaust velocity to vary across the range from chemical reactions (approximately 5km/s) to much higher values easily reaching 50 km/s. 10 000K ion temperatures are readily created by a laser pulse. Exhaust velocity is only a matter of intensity [11]. Thrust can be varied independently of v_E by changing the laser pulse repetition rate.

3.1 Pulsed Laser Ablation Propulsion

Ablation efficiency is defined as in Eq. (3) where u is drift velocity:

$$\psi = \langle v_x^2 \rangle / \langle v_x \rangle^2 = (u^2 + 2kT / m_e) / u^2 \quad (4)$$

This parameter ψ is the result of the fact that the exhaust velocity distribution is a drifting maxwellian with a nonzero mean velocity. However, it can be shown [12] that high intensity ablation plumes correspond to $\psi \leq 1.15$, and we will assume $\psi=1$ for simplicity in discussing efficiency. If ψ is larger, Eq. (3) shows it's a bonus for η_{AB} .

The change in velocity of the target from a single pulse is

$$\delta v_T = C_m \Phi / \mu_T \quad (5)$$

and

$$\delta v_{T\parallel} = \eta_c C_m \Phi / \mu_T \quad (6)$$

In Eqs. (5-6), μ_T is the target's areal mass density, η_c is an average geometrical efficiency factor taking account of the shape of the target and the fact that the ablation jet will be normal to each facet of its surface, not necessarily antiparallel to the laser beam. The quantity $\delta v_{T\parallel}$ is the change in target velocity in the beam direction. Eq. (6) is a numerically convenient formulation for space applications because we can deliver a fluence Φ to a region with diameter d_s and be sure that any object within that circle having mass density μ_T and the same C_m will gain the same velocity increment from the pulse. This is valid because space debris tend to exist in families with similar μ_T . For direct comparison to electric propulsion engines, the thrust to electrical power ratio is

$$C_{me} = \eta_{eo} C_m. \quad (7)$$

Laser electrical-to-optical efficiency η_{eo} can range from 25-80%, depending on the laser type. Exhaust velocity can be determined from the product of the easily measured quantities C_m and Q (J/kg ablated) as follows. Where

$$Q = W / \delta m_T = \Phi / \delta \mu_T, \quad (8)$$

it can be seen dimensionally that the product $C_m Q$ must be velocity:

$$v_E = C_m Q. \quad (9)$$

Note that $\delta \mu_T = \delta \mu_E$ by mass conservation. Eq. (9) can be extended to show that *ablation efficiency* is given by

$$\eta_{AB} = C_m v_E / 2 = \delta \mu_E v_E^2 / (2\Phi) = C_m I_{sp} g_o / 2, \quad (10)$$

where g_o is the acceleration of gravity and I_{sp} is the so-called specific impulse. C_m and I_{sp} are a constant product in which I_{sp} varies inversely with C_m for engines with the same efficiency. The units of I_{sp} are seconds. Another constant product is

$$C_m^2 Q / 2 = \eta_{AB}. \quad (11)$$

Because $\delta \mu_T = \rho_T \delta x$, the thickness of the solid target material ablated in one pulse is

$$\delta x = C_m^2 \Phi / (2\rho_T \eta_{AB}) \quad (12)$$

and fuel use rate is [2]

$$\dot{m} = \frac{2P\eta_{AB}}{(g_o I_{sp})^2}. \quad (13)$$

This can equivalently be written

$$\dot{m} = \frac{PC_m^2}{2\eta_{AB}} \quad (14)$$

In [2], we took $\eta_{AB}=1$ for simplicity and because I_{sp} was not measured for many materials. This is still true, because it is difficult to measure.

But we can play a trick: if we write

$$C_m = C_{mo} \eta_{AB} \quad (15)$$

and

$$P = P_o / \eta_{AB}, \quad (16)$$

Eq. (14) for fuel use rate becomes

$$\dot{m} = \frac{P_o C_{mo}^2}{2}, \quad (17)$$

a constant as η_{AB} varies, as is thrust, $F = PC_m$. The rate of material ablation is very small. As an example, for an aluminum target (density $\rho_T = 2700 \text{ kg/m}^3$), if $C_m = 70 \text{ N/MW}$, $\Phi = 35 \text{ kJ/m}^2$ and $\eta_{AB} = 1$, Eq. (12) gives $\delta x = 32 \text{ nm}$. At laser repetition frequency $f = 50 \text{ Hz}$, even in one minute operation, total ablation depth is $95 \mu\text{m}$. We assume a perfectly uniform beam, such as is achievable with modern methods of apodization.

In the laser propulsion examples given in Figures 9–10 and Table 3, laser average power is $5 \text{ MW} / \eta_{AB}$. It increases as η_{AB} decreases, and C_m decreases in the same ratio, so that thrust $F = PC_m$ and fuel usage rate are constant. Future measurements will tell us what η_{AB} is.

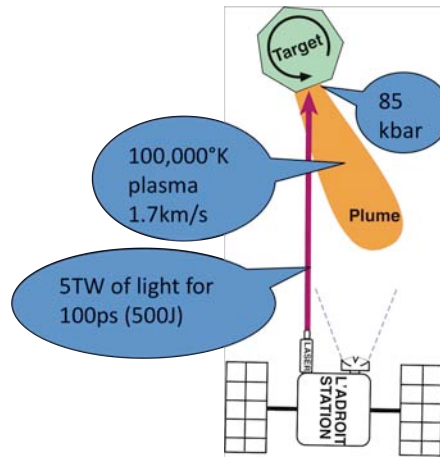


Figure 2. The figure illustrates that the plasma jet is always perpendicular to the irradiated surface, and shows examples for temperatures and pressures in plasma that can be achieved by an ultrashort-pulse laser interacting with a target in space.

3.2 Optima

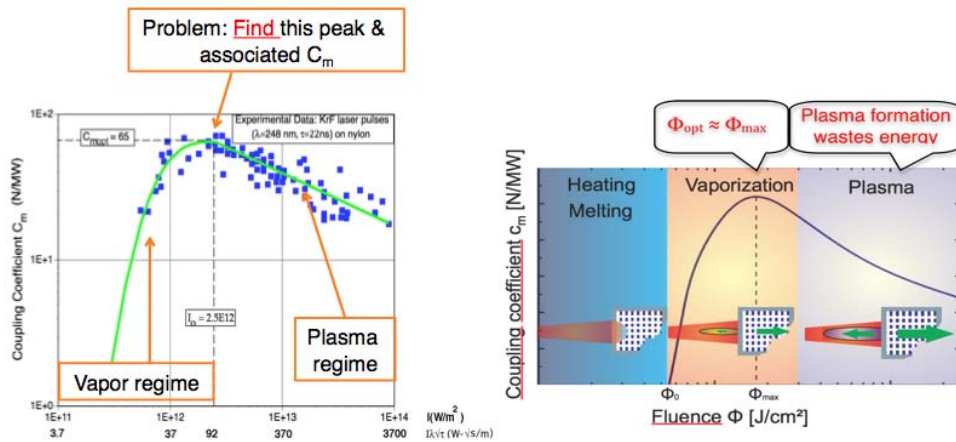


Figure 3. Illustrating C_{mopt} and $\Phi_{opt} = I_{opt} \tau$. Clearly both vapor and plasma regime must be considered in theory to find the optimum

A first optimum is the fluence which gives maximum C_m . Figure 3 shows [13, 14] experimental and notional plots of C_m values vs. incident fluence Φ to illustrate this optimum. In previous work, we called this C_m value and the fluence at which it occurs C_{mopt} and Φ_{opt} .

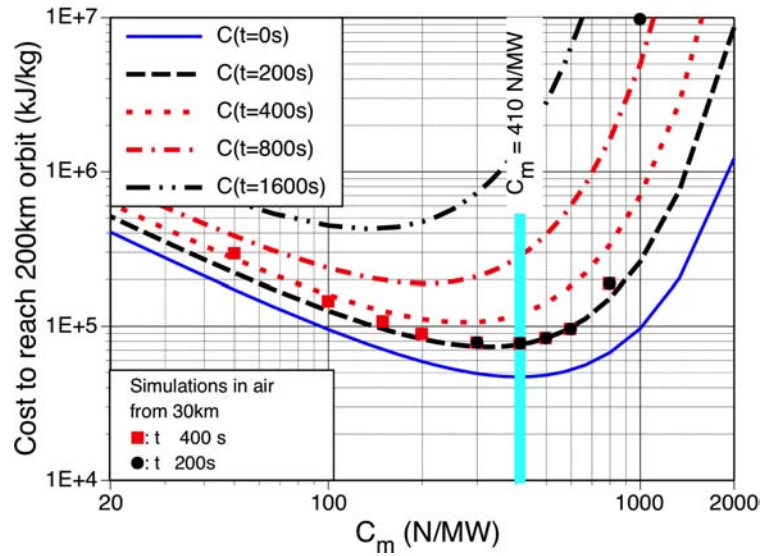


Figure 4. Results from simulations of laser-powered flights to LEO [2] (with different assumptions than the present work) show that each mission has an optimum-cost impulse coupling coefficient. Lines are theory, dots are simulations for a real atmosphere. Flight time depends on laser power. Black dot at the upper right shows that $C_m=1000$ N/MW gives infinite cost, i.e., the craft never reaches orbit.

We also showed another kind of optimum which gives minimum energy cost to complete a mission. From the figure, it is clear that $C_m=1000$ N/MW has an infinite cost for a 200s flight. The purpose of Figure 5 from [2] is to illustrate these optima. In [2], initial masses were 10 and 20.4kg. Delivered payload mass was 6.1kg. In the present work, we are not trying to minimize energy expenditure. Instead, we are trying to achieve absolute maximum payload mass fraction delivered at the end of the mission. Initial mass is 25kg and delivered mass as large as 13.5kg

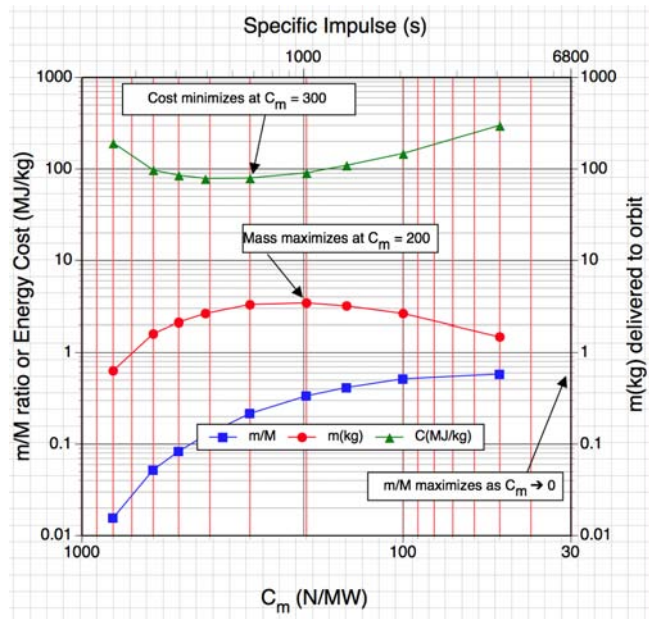


Figure 5. Results of many simulations in [2] showing that mass, mass ratio and cost optimize at different values of the coupling coefficient C_m . The figure shows the mass ratio m/M of delivered mass m to launch mass M maximizes at $C_m=0$ [$v_E=\infty$], mass delivered to LEO maximizes at $C_m=200$ N/MW ($v_E=10$ km/s), and cost minimizes at $C_m=300 - 400$ N/MW. We assumed $\eta_{AB}=1$, so exit velocity is $v_E=2/C_m$. These optima are specific to the ref. [2] case.

In [2], delivered mass ratios were much lower than in the present work because we limited consideration to $P=1\text{MW}$, requiring larger C_m to counteract gravity and smaller zenith angles. In consequence, different optima are realized than in this work. Our work in laser propulsion is to find lasers and materials which achieve a desired optimum.

4. New Results: DIY Coupling Coefficient

Table 1. New Coupling Results (1057nm)

Material \Rightarrow	Al		POM	
Pulsewidth	$C_m(\text{N/MW})$	$F(\text{kJ/m}^2)$	$C_m(\text{N/MW})$	$\Phi(\text{kJ/m}^2)$
400fs	28 ± 3	50 ± 20	125 ± 12	32 ± 6
80ps	28 ± 3	30 ± 7	773 ± 70	40 ± 8

In experiments conducted at École Polytechnique [15], we measured C_m on several materials at 400fs and 80ps, 1057nm. In the future we will repeat the measurements at 528nm, which may be more favorable for C_m . For our purposes, the most important results were for Al and POM (polyoxymethylene, Delrin[®]). The latter material gave very large C_m at 10.6 μm with the Myrabo [16] flyer, which achieved a flight altitude of 72m in air in 2000 [17]. We also found very high C_m for this material at 1057nm, 80ps [Table 1]. The same was not true at 400fs.

The POM C_m is too large for most laser launch projects [see Figure 4], but it is very useful in this way: we can now cast ablation fuel from a mixture of Al dust and POM to obtain any value we want in the range from 30 to 770N/MW at 80ps. As an example, an Al/POM mixture of 5% POM and 95% Al gives $C_m=70\text{N/MW}$. Density of the combination is 2640kg/m³, only slightly different from that of Al. The required fluence ($\sim 30\text{kJ/m}^2$) is about the same for both materials. For various reasons having to do with currently available laser system designs capable of 100 to 1kJ pulses, 400fs pulse duration is not attractive compared to 80ps, so it doesn't concern us that $C_{m\text{opt}}$ for POM at 400fs is much less than at 80ps.

Figure 6 shows our flyer design, both for launch to LEO and for interplanetary travel (next section). For the two cases, the ablator shell will have different C_m values. For LEO launch through the atmosphere, as we will see, C_m will be in the range 110-150N/MW, while for interplanetary travel $C_m=70\text{N/MW}$. As we will show, a craft designed to do both would have two layers: high C_m to get to LEO and low C_m , for the interplanetary portion of the flight.

5. Laser Launch to LEO

In [2], our method of laser-launching an object to low Earth orbit (LEO) was to separate the problem into two parts. First, we drove vertically through the atmosphere to altitude h_o , leaving a vertical velocity v_{ro} . Then, a second laser located at an appropriate distance to satisfy the geometrical constraints applied as much tangential thrust as possible to achieve orbit. This was too complex. Figures 7 and 8 show the launch geometry for this paper.

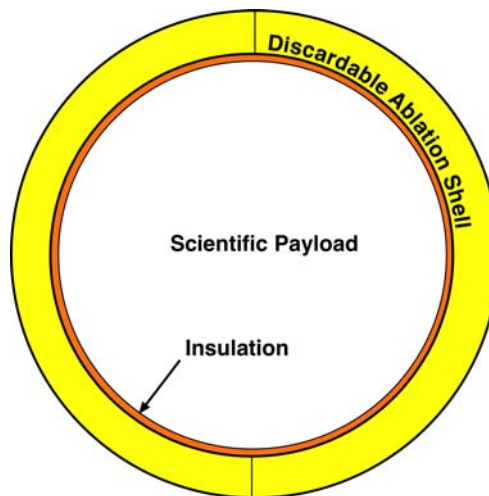


Figure 6. Laser-propelled flyer construction. Diameter is 50cm. The craft is rotating about all three axes at random frequencies. All elements of the surface have equal exposure to the laser beam. A small canister and gas jets produce and maintain the rotations during launch. The mass of the insulation and discardable shell holding the ablator is assumed to be 0.5kg.

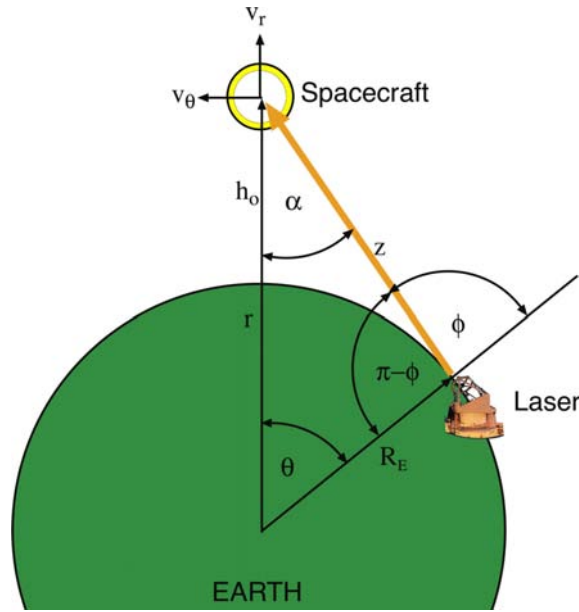


Figure 7. Geometry of Laser Launch to LEO.

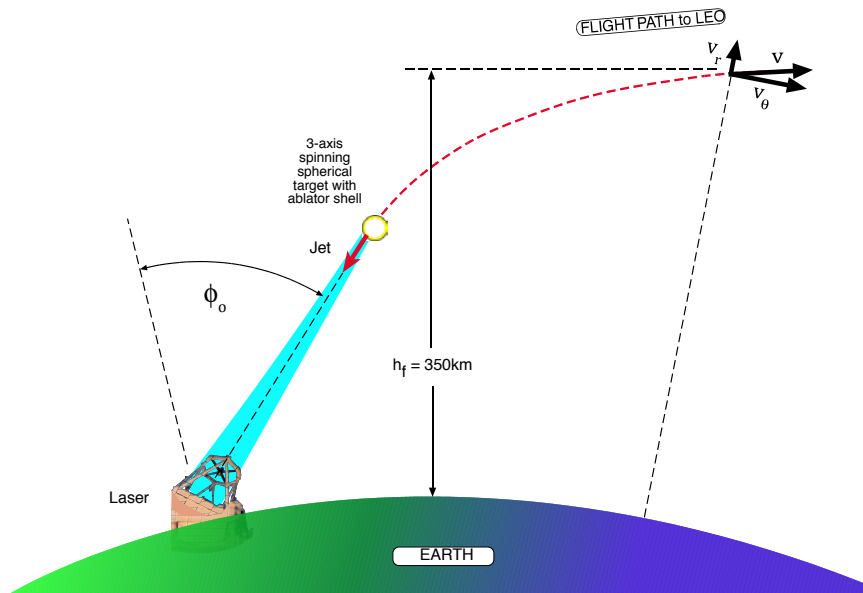


Figure 8. Laser station raises the target to 350km in one launch

5.1 Equations of Motion

Figures 7 and 8 show the geometry for launch from Earth to LEO. Here, we include atmospheric drag in the simulations. Referring to Figure 7 for the symbols, we note that

$$\cos \alpha = \frac{r^2 + z^2 - R_E^2}{2rz} \quad (18)$$

and that the tangential force on the spacecraft from incident laser power P is

$$F_\theta = PC_m \sin \alpha, \quad \text{where} \quad (19)$$

$$F = PC_m = \dot{m}v_E \quad \text{is the total force.} \quad (20)$$

Because
$$\dot{L} = m(r\dot{v}_\theta + \dot{r}v_\theta) = F_{\theta_{net}} r = \text{torque} \quad (22)$$

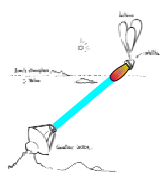





With drag,
$$F_{\theta_{net}} = (F - C_d A \rho v^2 / 2) \sin \alpha - m[\dot{v}_\theta + (\dot{r}/r)v_\theta] = m\dot{v}_\theta, \quad (23)$$

$$F_{r_{net}} = (F - C_d A \rho v^2) \cos \alpha + m[v_\theta^2 / r - g_o R_E^2 / (R_E + h)^2] = m\dot{v}_r. \quad (24)$$

$A = (\pi D_p^2 / 4)$ is the exposed cross section area of the spherical probe, $\rho(h)$ is the atmospheric density – an exponential with scale height 7km – at altitude h and v^2 is the sum square of the radial and tangential velocities. In Eqs. (20)-(25), all quantities except the obvious constants are functions of time. η_c is a structural efficiency factor to account for the spacial average of the ablation thrust vector, which we take to be 0.8. C_d is the drag coefficient, v_r is vertical velocity, μ is the target areal mass areal density (to match the dimensions of Φ), P is total laser power on target, f is pulse repetition frequency and D_p is the target diameter.

5.2 Initial Target Altitude and Ways to Achieve it

Table 2. Ways to achieve initial target altitude above denser part of atmosphere

Method	Problems	Additional Est. Cost
	Balloon to 35km <ul style="list-style-type: none"> Uncontrolled target position at laser turnon To launch 6 targets, 9,900 m³ volume \$45k helium cost Helium is a precious resource 	\$300/kg
	Very large gun <ul style="list-style-type: none"> 1000 G's Acceleration Need 1kms muzzle velocity Facility cost dominant Noise, gov't opposition 	\$200/kg
	Loitering jet plane <ul style="list-style-type: none"> \$3k\$/hr cost 12km max altitude 4 hrs/fuel load 8-target load at 50/day 	\$60/kg to 12km
	Black Brant Rocket <ul style="list-style-type: none"> One flight per target \$600k/launch 	\$2,400/kg
	8km tower <ul style="list-style-type: none"> Uncertain development cost Uncertain stability 8km not enough to help much 	Uncertain
	Laser <ul style="list-style-type: none"> Combusting target in atmosphere Penalty on laser energy at lower launch altitude 	Zero additional cost

5.3 Launch Strategy

There are a large number of interacting factors involving C_m , time, laser range, laser power, delivered mass fraction, final elevation angle, minimum altitude, insertion altitude and total propagation range with the geometry of Figure 8. Finding an optimum combination is a matter of art. We found that whatever you do with a laser on the earth's surface, even with the 5MW average power rep-pulse laser which we used here, it is easy to have the target disappear over the horizon before insertion as well as for it to have an undesirable amount of residual radial velocity. Best performance was obtained with $C_m=120 - 150$ N/MW. This choice increases I_{sp} and fuel lifetime.

5.4 Orbital Insertion

In the Figure 9 flight (Case 5 of Table 3), we launched from 35 km altitude to minimize energy expended in drag. Even so, only 28% of the mass survived into LEO. The question of how best to get to 35km still remains (Table 2). We were not able to launch from the ground in any single-power flight. In Figure 10 (case 3), beginning at 1 km altitude also involved significant loss to drag: delivered mass ratio was 38%, despite the 35 km launch altitude. To avoid excessive v_{rf} in a single-power flight, the beam elevation angle must be small, leading to high drag in case 5.

Table 3. Launch summary. Common parameter: $P=5\text{MW}/\eta_{AB}$. P doubles or triples at end.

Case	C_m/η_{AB} (N/MW)	Chord (km)	T (s)	T_{pk} drag	$\phi_o(^{\circ})$	$\phi_f(^{\circ})$	a_{max} (m/s ²)	v_{rf} (km/s)	m_f/M (%)	h_o (km)	h_p (km)	h_a (km)	s_f (km)
3A	150	1.5	402	60	56	84	173	0.25	38	1	96	842	1030
5	130	61	429	55	60	90	47	1.47	28	35	112	10000	1680
11	110	15	540	30	45.5	89	52	0.70	52	15	409	4480	1190
11A	110	15	485	30	45.5	89	173	0.069	61	15	112	926	824
11B	120	1	496	10	45.5	90	216	0.39	54	1	104	41700	873

In Table 3, “Chord” is the horizontal distance from the laser station to the point beneath the satellite at launch. T is flight duration. T_{pkdrag} is the time at which drag is maximized. ϕ_o and ϕ_f are initial and final zenith angles, h_o , h_p and h_a initial, perigee and apogee altitudes, v_{rf} final radial velocity and s_f final laser range to the spacecraft. a_{max} is maximum acceleration. m is mass delivered to orbit and M is mass on the ground.

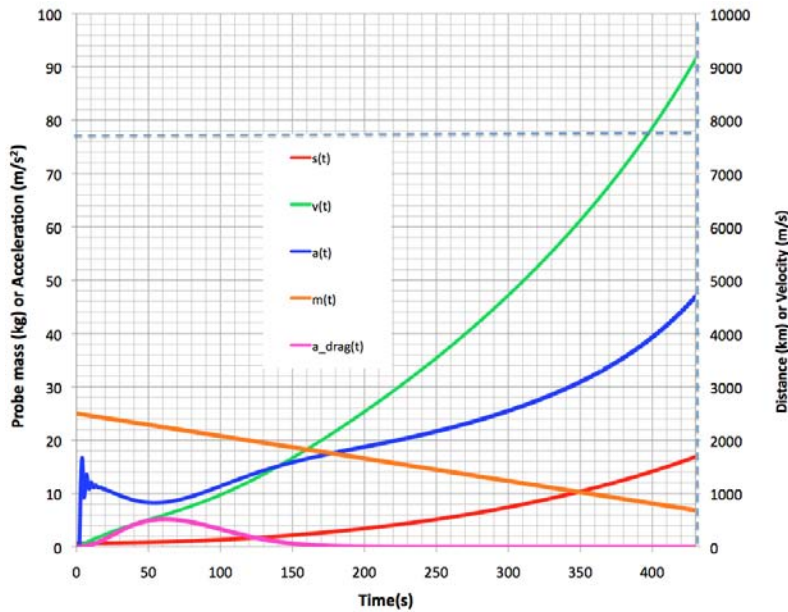


Figure 9. Case 5. Our only single-power laser launch, from 35km altitude to LEO with $C_m=130$ N/MW. Laser is shut off at 429s. $s(t)$ is laser range. Altitude at insertion is 409 km. Initial zenith angle is 60° and final zenith angle is 90° . Drag loss is significant, so mass ratio delivered to orbit is 28%. With final radial velocity 1.47km/s and final velocity 9.09km/s, vector velocity slope at insertion is acceptable (9.3°) for a successful orbit. Apogee is 10000 km.

In these flights, velocity v is the root square sum of the radial and tangential components. Because of extreme orbit sensitivity to the radial velocity component, initial zenith angle and other parameters, we found, in general, that a two-phase flight was necessary to obtain a good orbit. To achieve $C_m=150\text{N/MW}$, the ablator was 15% POM and

84% Al, with density 2500 kg/m^3 . Table 3 shows numerical parameters for 5 selected flights that achieved orbit with the most interesting results for each situation.

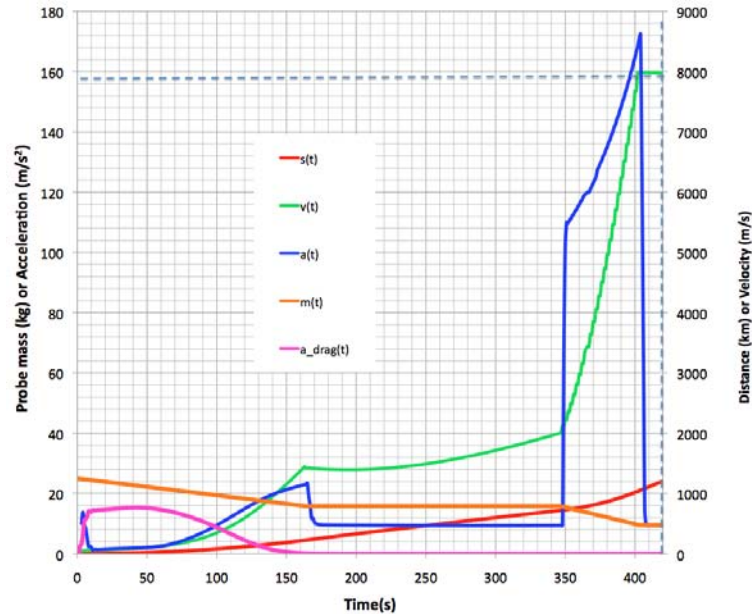


Figure 10. Case 3A. Laser-launch from 1km altitude lasting 160s at 5MW gets us above the atmosphere quickly. Then, a 180s coast followed by a 10MW burst in the last 60s gets us into LEO. $C_m=150\text{N/MW}$. Initial zenith angle is 56° , final zenith angle 90° , mass ratio delivered to orbit 38%. Final radial velocity is 238m/s and final velocity 7.98 km/s . Perigee 100km , apogee 838km and final zenith angle 90° . Too much loss to drag. Insertion slope is 1.7° .

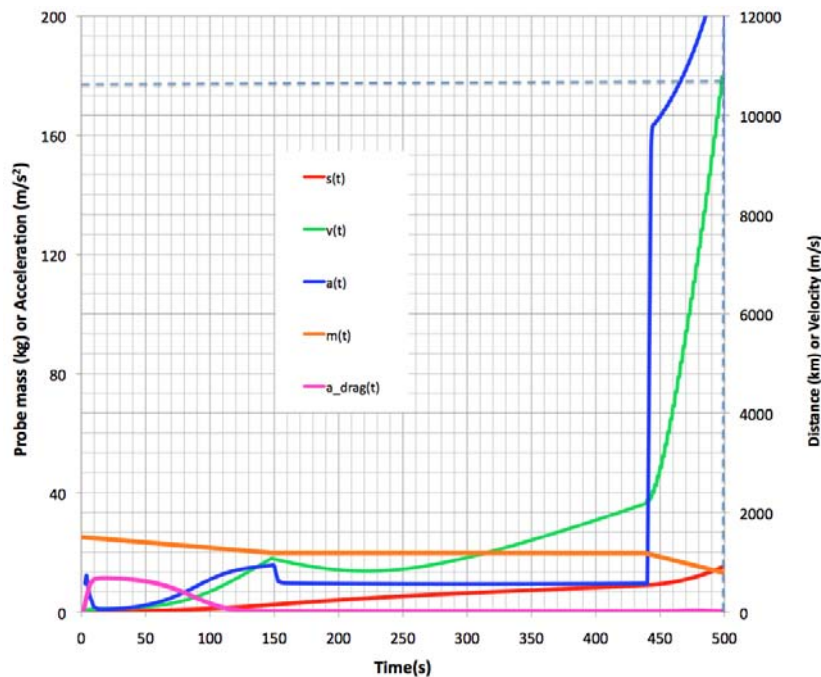


Figure 11. Case 11B. Fascinating launch from ground (1km altitude) with $C_m=120\text{N/MW}$. A 300s coast followed by a 15MW burst during 60s at the very end gets our craft into orbit. This profile gives m/M delivered to orbit of 54% (13.5kg). Initial zenith angle 45.5° , final zenith angle 90° . Final radial velocity is 389m/s , final velocity 10.4km/s . Perigee 104km , apogee $41,700 \text{ km}$, 117% of geosynchronous altitude. Insertion slope is 2.12° . Minimal energy is wasted in drag, even though we are starting from the ground. Applications are to GEO satellite inspection.

In our simulations, initial target altitudes were chosen as 1, 10, 15 and 35km. Laser beam range was always $<2000 \text{ km}$. The laser station is assumed to be located at 3km altitude on a mountain so that large zenith angles are manageable. Acceleration was always reasonable. Delivered mass fraction was very impressive. Contrary to our

expectations, launching directly through the atmosphere, rather than popping straight up and then pushing tangentially to insertion, had better results than in [2]. Figure 11 shows that a 45° initial zenith angle is permitted in a 3-phase complex flight profile [Table 3, Case 11B]. In other cases, a much larger initial zenith angle was required to minimize radial velocity at insertion.

5.5 Lasers

Table 4. Laser and target parameters

Type	Diode-pumped Nd
Wavelength	1057nm for ground launch, 532nm in space
Pulse duration	100ps
Pulse energy	5kJ
Pulse repetition rate	250Hz/1kHz/2kHz/3kHz
Laser average power P_o	1.25 - 15MW
Target initial mass m	25kg
C_{mo}	Various, 70-150N/MW
D_b (Mirror diameter)	6m/3m

Laser parameters assumed in this work are listed in Table 4. Such high repetition rate, high pulse energy lasers are not yet demonstrated, but are being developed. The state of the art in the lasers we currently need to achieve all of these applications is represented in the HiLASE program [18], where the Rutherford Appleton Laboratory's "DiPOLE 100" laser achieved its full design performance of 1kW average power with 10Hz, 100J pulses at 10ns pulse duration. We prefer 1057nm for the wavelength in atmosphere because absorption is greater at the second and third harmonics, especially at low elevation angles. In space, 355nm is ideal. For energy storage, 6GJ, 15MW super batteries using zinc hybrid cathode technology have now been developed [19]. These batteries can be totally discharged without lifetime penalty. Because 10% discharge/recharge is the rule for most other battery types to ensure long life, this development increases battery mass efficiency by an order of magnitude.

5.6 Discussion

Why are the results here so much better than in [2]? The main reason is that much larger laser power allows us to oppose gravity with smaller C_m , and this leads to higher I_{sp} and longer fuel life [Eq. (13)]. Higher temperature gives larger mass velocity in the laser-produced jet. Having 300% of normal power available in a burst at the end of the flight also vastly improves mass delivery, as we show in Case 11B (Table 3). This is our best case for a flight from the ground, with 54% of mass delivered to LEO (1km starting altitude). Table 3 also shows that m/M of 61% is possible from a 15km starting altitude.

To choose the best flight parameters, there are additional constraints: considering diffraction, scintillation and adaptive optics, maximum permissible range is 2000 km for 1060nm and a 6-m mirror.

The reason for the inevitable radial velocity can be seen in Figure 7. Even if ϕ is 90° , it is still true that $\alpha < 90^\circ$, so unavoidable radial momentum is delivered by the laser beam. In Case 11B, $\alpha = 45.5^\circ$ at the beginning, but 82° at the flight's end. The key to successful flights is that thrust applied toward the very end is more effective than thrust applied earlier in avoiding unwanted radial velocity. Radial velocity gives poorer orbits and less overall efficiency, or even a crash at perigee.

5.7 Energy Cost Perspective

For the simulations reported in Figure 5 from [2], the minimum emitted laser beam energy cost per kg delivered to orbit was 80MJ/kg. In case 11B, this cost was 120 MJ/kg. In [2], we assumed perfect alignment of the beam with the target trajectory, which was supposed to have been achieved with a guidance system and tilting reflectors on the tail of the flyer. In this work, we use a more realistic target that always provides reaction along the beam axis without special mirrors or guidance, but the thrust vector is not perfectly aligned with the path to orbit. This probably explains the difference. The inherent total energy change to create the orbits in Table 3 vary from about 2.4 MJ/kg to 24 MJ/kg. Riding an elevator to 150 km amounts to 1.5 MJ/kg. A bullet with 7.98 km/s velocity contains 32 MJ/kg. The parameter Q in Eq. (8) is related to, but incommensurate with, all these values, because it relates to the mass ablated rather than the mass delivered. Q derived from Eq. (11) for a typical flight at 120 N/MW is 140 MJ/kg.

6.0 Laser-powered Rockets

In this section, we consider a laser-propelled rocket, consisting of the Figure 6 flyer. Flight trajectory is shown in Figure 12. This is an instantaneous launch, from the point of view of the astrodynamics. Here, we don't have to worry about minimum perigee.

6.1 Equations of Motion

The equation of motion in this case is very simple:

$$\ddot{s} = \frac{PC_m \eta_c}{m} \quad (25)$$

because there is no drag. The laser and the target are in a micro-G environment in LEO, not on the ground. Because an object launched from LEO as shown in Figure 13 needs a Δv of 3.6km/s to reach its goal, our only problem is to generate this Δv , rather than worrying about the detailed gravity fields of Earth and the Sun between LEO and Mars. Earth and Sun gravity influence the flight along the way, but all we need to know at the outset is the required Δv and pointing direction, and to deliver it quickly. A flight result is shown in Figure 13. Initial mass fraction delivered to Mars is 73%.

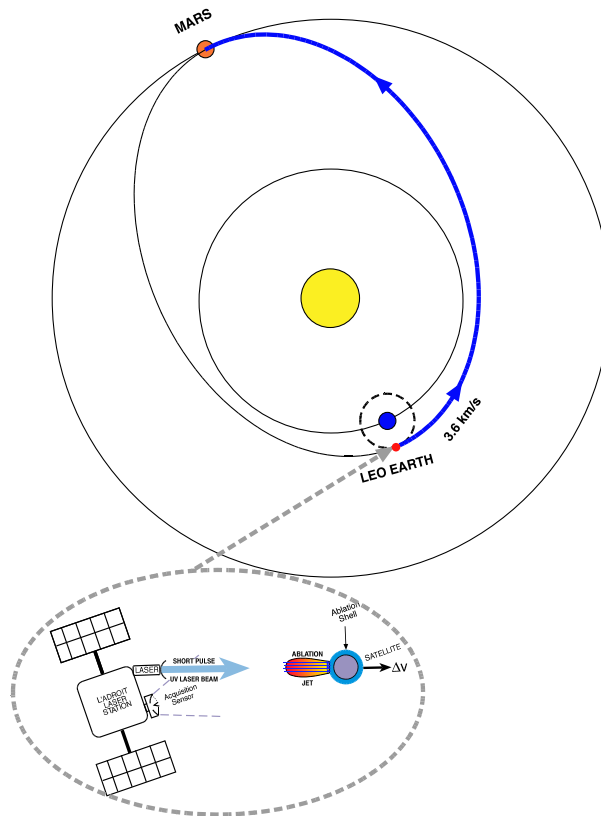


Figure 12. A cis-Mars trajectory starting from LEO requires $\Delta v=3.6\text{km/s}$.

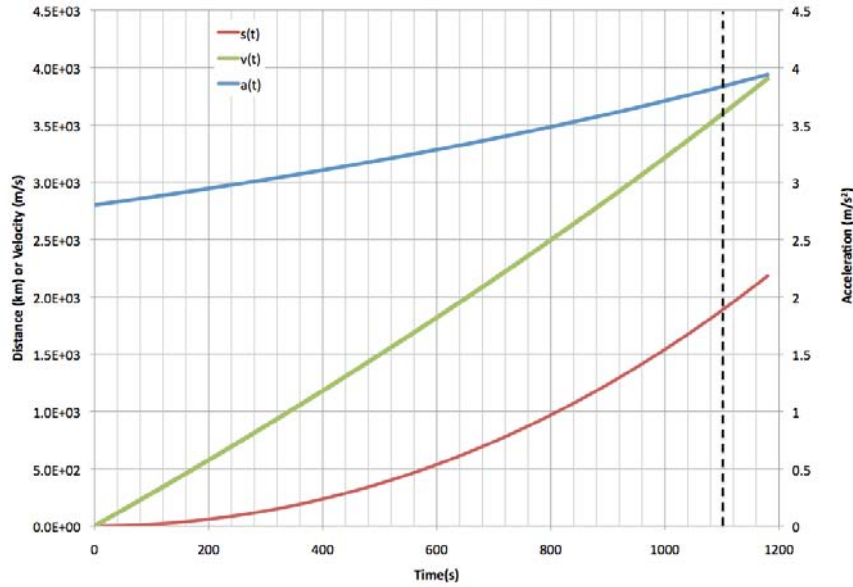


Figure 13. The necessary velocity of 3.6 km/s is obtained after accelerating for 18.5 minutes, and 18.2 kg is delivered to the cis-Mars trajectory.

6.2 Discussion

The laser-powered rocket is an exciting project for future research. We were pleased that our analysis showed 73% of initial mass could be delivered to a Mars trajectory from LEO. Even better, the laser is only 1.25 MW, not 5, and can be the third Nd harmonic (355 nm) in space. For this reason the mirror can have 3 m diameter rather than 6 m, as in the LEO launch analysis. Although C_m and I_{sp} have not been measured at 355 nm, theory [ref. (3)] says C_m should be better at the shorter wavelength. We remind the reader that the laser power and C_m values listed in Table 5 should be understood to be adjusted according to Eqs. (15)–(16) when ablation efficiencies are known. If such a flight were concatenated with a maximally efficient launch from ground to LEO, total mass fraction would be 39%. It is clear that we could launch to Mars directly from the Earth with groundbased and spacebased lasers, but that's another paper!

Table 5. Parameters for flight to Mars

Wavelength (nm)	355
Pulse duration (ps)	100
Pulse energy (kJ)	5
Repetition rate (Hz)	250
Average power (MW)	1.25
C_m (N/MW)	70
Fluence Φ (kJ/m²)	35
Target diameter (cm)	50
Initial mass (kg)	25
Final mass (kg)	18.2 (73%)
Final velocity (km/s)	3.6
Acceleration time (min)	18.5
Mirror diameter (m)	3
Maximum range (km)	1900
Maximum acceleration (m/s²)	3.84
Ablation efficiency	1.0

7.0 Conclusions

For several years, scientists have been launching thin foils with short-pulse lasers to 8km/s velocities [20]. A way to understand the work reported here is that we launch the equivalent of 400,000 or so thin foils at similar velocities toward the laser beam, one at a time, and the reaction momentum propels a craft in space efficiently.

For the first time, we showed it is possible to laser launch directly from the Earth's surface, and still obtain excellent mass fraction m/M of as large as 54% delivered to LEO. This is more than a factor-of-10 improvement over state of the art m/M ratios with chemical rockets. This, an exciting result of this study, can be utilized by assembling larger stations on orbit from pieces, or for launching swarms of micro- or nanosatellites at low cost.

We used a novel design in which a sphere covered with ablation fuel is caused to rotate randomly so that the entire surface is used for fuel, creating a jet which is always directed opposite to the laser beam. Rotation is presumed to be caused by, e.g., gas jets from a small internal canister. The direction of the beam itself governs the direction of the sphere's trajectory.

These are all passive ablation fuels. As we showed in [11], it is possible to obtain 3-4 times larger C_m with energetic materials like glycidyl azide polymer (GAP).

In the absence of accurate data on specific impulse I_{sp} for our target materials, we showed that it is still possible to use a scaling with laser power inversely proportional to η_{AB} and coupling coefficient C_m proportional to η_{AB} to provide constant thrust and fuel lifetime.

Flight times to LEO were 250 – 540s. Laser power was $5\text{MW}/\eta_{AB}$ and the probe initial mass was 25kg. In the best cases, a burst of 10-15 MW/η_{AB} was applied in the last 80s, producing a significant increase in m/M as well as a better values for final orbit parameters.

If a practical, low-cost way (balloon, gun, tall tower) is developed to lift the flyers to 15km before laser acceleration, we showed even better m/M values for the overall flight. The cost of doing this may not be worthwhile. The gains for initiating the flight at 35km rather than 15km are probably not worth the additional effort.

Our calculations show that this technology, combined with a 1B\$ groundbased laser station capable of 30 launches/day, can reduce launch costs to LEO to about \$300/kg, a factor of 30 below present experience.

An important application of this work is to launching constellations of Earth-observing microsatellites, to more carefully monitor global climate change and its consequences, in order to spot trends at the earliest possible time and to develop very highly detailed global models. Another application is to sending inspection craft to geosynchronous (GEO) orbit.

The second important result of this work is that it is not difficult to send a probe to Mars in a year or so, with 73% of the mass surviving. Laser wavelength should be the Nd 3^{rd} harmonic in this case (355nm) because of its better C_m and lower divergence, making possible smaller mirrors than for the LEO launch case. Maximum laser range was 2000km.

Further applications of this work are to longer flights within the solar system on one extreme of difficulty, and to placing satellites in LEO or GEO orbits on the other. As higher power lasers are developed, larger masses than 25kg can also be laser-launched.

8.0 Acronyms and Abbreviations

Table 6. Acronyms and abbreviations used in this work

CEA	Commissariat à l'Énergie Atomique et aux Énergies Alternatives
CEMEF	Centre de Mise en Forme des Matériaux
CESTA	Centre d'Études Scientifiques et Techniques d'Aquitaine
CNES	Centre National d'Études Spatiales
CNRS	Centre National de la Recherche Scientifique
DAM	Direction des Applications Militaires
DIF	DAM Île-de-France
DiPOLE	High repetition rate laser developed by the Rutherford Appleton Laboratory

DIY	Do-it-yourself
GAP	Glycidyl azide polymer
GEO	Geosynchronous orbit
HiLASE	High repetition rate European Union laser project in the Czech Republic
IKAROS	Interplanetary Kite-craft Accelerated by Radiation of the Sun
JAXA	Japan Aerospace Exploration Agency
LEO	Low Earth Orbit
LLC	Limited Liability Corporation
LULI	Laboratoire pour l'Utilisation des Lasers Intenses (École Polytechnique)
Nd	Neodymium lasing medium in glass or other host
POM	Polyoxymethylene, trade name Delrin®

References

- [1] C. Phipps and M. Michaelis, "LISP," *J. Laser and Particle Beams*, **12** (1), 23-54 (1994)
- [2] C. Phipps, J. Reilly and J. Campbell, "Optimum Parameters for Laser-launching Objects into Low Earth Orbit," *J. Laser and Particle Beams*, **18** (4), 661-695 (2000)
- [3] C. Phipps and C. Bonnal, "A spaceborne, pulsed UV laser system for re-entering or nudging LEO debris, and re-orbiting GEO debris," *Acta Astronautica*, **118**, 224-236 (2016)
- [4] F. Tsander, "Flight to other planets," (1924) in Ye. Moshkin, *Development of Russian Rocket Technology*, Mashinostroyeniye Press, Moscow (1973) (in Russian)
- [5] K. Tsiolkovsky, "Plan of Space Exploration". 1926 (in Russian), available in English in "Exploration of the Universe with Reaction Machines: Exploring the Unknown," NASA History Series. NASA SP 4407, Washington, D.C. (1995)
- [6] H. Oberth, "Die Rakete zu den Planetenräumen", (The Rocket to the Planet Spaces) Oldenbourg Verlag, München (1923)
- [7] E. Sänger, "Zur Theorie der Photonenraketen," Probleme der Weltraumforschung (IV. Internationaler Astronautischer Kongress, Zürich 1953; S. 32, Biel-Bienne: Laubscher (1955)
- [8] C. Phipps, "Pulsed lasers for clearing debris in LEO and GEO," *Proc. LSSE Conference*, Yokohama, 17-20 May 2016
- [9] C. Phipps, et al., "Review: Laser Ablation Propulsion," *J. Propulsion and Power*, **26** no. 4 pp. 609-637 (2010)
- [10] H. Yano, "Cosmic dust detection by the IKAROS large area dust detectors ion interplanetary space from the Earth to Venus," *42nd Lunar and Planetary Science Conference* (2011) [in Japanese]
- [11] C. Phipps, J. Luke and W. Helgeson, "Laser-powered, multi-newton thrust space engine with variable specific impulse," *High-Power Laser Ablation VII, Proceedings of SPIE* **7005**, 1X1-1X-8 (2008)
- [12] C. R. Phipps and J. R. Luke, "Laser Space Propulsion," *Laser Ablation and its Applications*, Chap.16, Springer, 407-434 (2007)
- [13] C. Phipps, et al. *Appl. Surf. Sci.* **252** (2006) 4838-4844
- [14] Courtesy of H.-A. Eckel, DLR Stuttgart
- [15] C. Phipps, M.Boustie, J.-M. Chevalier, S. Baton, E. Bambrink, L. Berthe, M. Schneider, L. Videau and S. Boyer, "Laser impulse coupling and ablated mass measurements at 400fs and 80ps using the LULI facility at 1057nm wavelength," *J. Appl. Phys.* In preparation
- [16] L. N. Myrabo, D. G. Messitt, F. B. Mead Jr., "Ground and flight tests of a laser propelled vehicle," paper AIAA 98-1001, 36th AIAA Aerospace Science Meeting & Exhibit, 12-15 January 1998, Reno, NV (1998)
- [17] L. N. Myrabo, "World Record Flights of Beam-Riding Rocket Lightcraft: Demonstration of 'Disruptive' Propulsion Technology," paper AIAA 2001-3798, 37th AIAA/ASME/SAE/ASEE Joint Propulsion Conference, 8-11 July 2001, Salt Lake City, UT (2001)
- [18] <http://www.hilase.cz/en/advanced-dpssl-laser-dipole-100-delivers-1kw-performance/>
- [19] <http://www.eosenergystorage.com/technology-and-products/>, page 2
- [20] Z. Gong, et al. "Experimental study for laser-driven flyer plates up to 8km/s," International Astronautical Federation paper IAC-15,A6,3,8,x29049 (2015)